

# Joint Centre for Mesoscale Meteorology, Reading, UK



## On the nature of the convective circulations at a kata-cold front;

K. A. Browning

Internal Report No. 35

September 1994

**Met Office** Joint Centre for Mesoscale Meteorology Department of Meteorology  
University of Reading PO Box 243 Reading RG6 6BB United Kingdom  
Tel: +44 (0)118 931 8425 Fax: +44 (0)118 931 8791  
[www.metoffice.com](http://www.metoffice.com)



**On the nature of the convective circulations  
at a kata-cold front**

**K A Browning\***

**University of Reading, UK**

---

**\*Corresponding address: Joint Centre for Mesoscale Meteorology, Harry Pitt Building, University of Reading, Whiteknights Road, PO Box 240, Reading RG6 2FN, UK. (The Joint Centre for Mesoscale Meteorology is supported by the Meteorological Office and the Department of Meteorology, University of Reading).**

## Abstract

A series of dropsondes released over the sea, with mesoscale spacing, is analysed to reveal the structure of a kata-cold front characterised broadly by a dry airstream over-running a warm moist boundary layer. The front had a multiple structure and this paper is concerned with the detailed structure of one of the surface cold fronts. Two kinds of circulations are shown to coexist: vertical convection and a slantwise circulation. The slantwise circulation is a feature not normally resolved by conventional observations of kata-cold fronts: it is shown to be a small-scale version of the rearward-sloping ascent encountered in ana-cold fronts. Much of the slantwise circulation was cloud-free but where it impinged upon the boundary layer it triggered the development of a narrow band of convective cloud, the tops of which extended downstream within air that was overtaking the front.

### 1. Introduction

The two main classes of cold front were classified by Sansom (1951) as either ana-fronts or kata-fronts according to whether ascending or descending airflows dominate their structure. Ana-cold fronts are characterised by rearward-sloping ascent of air with high wet-bulb potential temperature ( $\theta_w$ ). Much of this warm air originates as a strong low-level flow just ahead of the surface cold front. The warm air ascends above the advancing wedge of cold air. In NW Europe, however, such fronts are rather less common than kata-cold fronts.

Kata-cold fronts are superficially quite different: in kata-cold frontal situations, the warm air (see solid arrow labelled Warm Conveyor Belt in Fig 1) ascends in advance of the

cold front and is overrun by dry, low- $\theta_w$  air (dashed arrow in Fig 1). This overrunning airstream originates in the upper troposphere or lower stratosphere and is known as the Dry Intrusion. The leading edge of the dry intrusion constitutes an upper cold front or moisture front. Because of this separation between the surface cold front (SCF) and upper cold front (UCF), kata-cold fronts are also referred to as split fronts (Browning and Monk, 1982).

A feature of kata-cold fronts, glossed over in the simple split front model, is the fine structure that occurs within the SCF part of the split front. As seen in satellite imagery, this often manifests itself as multiple, rather shallow and narrow, cloud bands. Each band corresponds to a slight local sharpening of the generally rather diffuse low-level cold frontal zone that characterises most kata-cold fronts.

The purpose of this paper is to present some exceptionally detailed observations of such a multiply-banded SCF and to derive a conceptual model of the dynamic and thermodynamic structure of one of the bands. A feature of the model is that two distinct kinds of circulation can coexist in association with a single SCF cloud band:

- (i) a small-scale slantwise circulation, and
- (ii) vertical convective cells.

In some respects the structure resembles that of an ana-cold front but on a much smaller scale. Both circulations are confined to the lowest 2.5km of the atmosphere and can be thought of almost as boundary layer phenomena. In the case studied, the cold air was travelling over a relatively warm sea surface and the boundary layer was convectively

unstable. We believe that our conceptual model may have implications for representing the mixing processes between such a convectively unstable boundary layer and the overlying free troposphere.

## 2. Context of the case study

The principal data used in this study are a sequence of dropsondes released by the Meteorological Research Flight C-130 aircraft in the vicinity of a frontal cyclone during the FRONTS-92 experiment. The experiment was undertaken over the open sea (NE Atlantic) and presented an opportunity to study frontal structure in the absence of the complicating effects of topography. The broad features of the 27 April case presented in this paper have been described by Browning et al (1994). Here we shall carry out a more detailed analysis of a small portion of the data, concentrating on part of a transect through a kata-cold front that displayed a multiply banded SCF. The criterion used by forecasters to classify a cold front as a kata-front is that the wind component ( $u$ ) normal to the front should increase with height in the warm air. Fig 2, depicting the vertical profile of  $u$  is consistent with this criterion.

Visible and infra-red satellite images for 1730 UTC on 27 April are shown in Fig 3. The line AB in Fig 3(b) shows the aircraft track, relative to the frontal system, during the period from 1618 (at location A on the cold side) to 1742 (at the location B on the warm side of the frontal zone). Between A and B the aircraft track took it over a number of shallow SCF cloud bands orientated SW-NE. Seventeen dropsondes were released between A and B, and the resulting pattern of relative humidity is shown in Fig 4.

Very dry, cold air (relative humidity between 10 and 20%) was advancing over a relatively warm ocean. The resulting convectively unstable boundary layer showed considerable variation in structure associated with the multiple SCF cloud bands. One feature to note in Fig 4 is the way in which dry fingers penetrated slantwise to quite low levels (along the dashed axes in Fig 4). Browning et al (1994) shows that the more well-defined fingers were laterally extensive and corresponded to corrugated laminae that were related to the banded cloud structures seen in the imagery. Two of these dry laminae penetrated to the surface where they gave rise to two surface cold fronts, labelled SCF1 and SCF 2 in Fig 4. We shall restrict our attention to SCF 1, especially the small rectangular inset drawn in Fig 4. The associated cloud band as determined from satellite imagery is shown in Fig 4 as C1.

### 3. Detailed mesoscale structure associated with SCF 1

#### (a) The slantwise circulation

Near SCF 1, within the small region shown framed in Fig 4, there were as many as 7 dropsondes, plus two more, slightly to one side of the section. Locations of all 9 sondes are shown by dots in Fig 3(b). The 3 northernmost sondes (Numbered 11, 12 and 13 in Fig 4) were above low cloud (tops at 1 km). The 5 southernmost sondes (Numbered 15 to 19) were close to the cloud band associated with SCF 1, the tops of which extended up to about 2.4km. In between, Sonde Number 14 fell through a cloud-free zone. This cloud-free zone shows up clearly as a dark strip in the visible imagery (Fig 3(a)).

The detailed dropsonde analysis for SCF 1, based on the above 9 sondes, is shown in Fig 5. Data have been plotted at height intervals of 80m, each value being a running average over about 500m (strictly 50mb). Figs 5(a) and (b) show aspects of the thermodynamic structure; shaded regions draw attention to regions of moist air ( $RH > 90\%$ ) and high  $\theta_w$  ( $> 11C$ ), respectively. Fig 5(c) shows the transverse wind component ( $u$ ), the shaded region corresponding to a minimum in  $u$ ; the front itself was propagating with a  $u$ -component of between 17 and 18  $m\ s^{-1}$  so that the shaded region was evidently a rearward-directed flow of up to 1  $m\ s^{-1}$  relative to the front. We are attributing significance to quite small features in the analysed fields. We have confidence in the validity of such details because corresponding features can be clearly identified within sequences of sondes both in the thermodynamic fields and in the independently-measured kinematic fields.

In order to clarify the inter-relationship between the various fields, the isopleths bounding each of the shaded regions in Figs 5(a), (b) and (c) are plotted together in Fig 5(d). What emerges is a picture of a moist lamina associated with a rearward-directed flow of air with a  $\theta_w$  of 11C. Taking into account the fact that the section AB was not quite normal to the cold frontal bands, the moist lamina is estimated to have been inclined at roughly 1 in 40. This is consistent with rearward-sloping ascent within it of about 2  $cm\ s^{-1}$ . Although the relative humidity in the moist lamina was high, it was generally subsaturated; indeed, except within about 10km of the surface front, this was the very region that was cloud-free in the imagery.

(b) The vertical convection

The satellite-detected cloud band associated with CF1 was situated mainly in advance of the position of the surface cold front. As sketched in Fig 5(d), this cloud had tops up to  $2.4 \text{ km} \pm 0.2 \text{ km}$ , at which level the dropsondes showed a layer of air with  $\theta_w = 12\text{C}$  that was characterised by slightly increased relative humidity. Fig 5(b) shows that this is consistent with the convective ascent of air parcels from near the surface to their convective equilibrium level. Once they reached this level, Fig 5(c) shows that they will have entered a region where the flow was overtaking the front at about  $2 \text{ m s}^{-1}$ . In fact there were also strong components of flow perpendicular to the plane of Fig 5 which we can examine via an analysis in plan view (Fig 6).

Fig 6 shows a tracing of the cloud band associated with CF1. The heavily stippled regions show deeper cloud (tops to about 2.4 km) embedded within a broader region of shallower cloud (lightly stippled). As often happens, the convective cloud tops extend downwind at an angle of about 20 deg to the overall frontal cloudband. Parts of the isentropic analyses for the  $\theta = 10\text{C}$  and  $25\text{C}$  surfaces, derived by Browning et al (1994), are superimposed on the satellite-derived cloud pattern in Fig 6. These show that the relative flow in the  $10\text{C}$   $\theta$ -surface just behind SCF 1 descended from the north and terminated behind the surface front. However, the relative flow in the  $25\text{C}$  surface descended toward the front from the northwest, and then veered, before crossing over the front just above the cloud tops and ascending toward the northeast. The flow at the level of the cloud tops behaved similarly. The convective cloud tops were aligned with this flow.

(c) Vertical mixing associated with the circulations

A simplified interpretation of Fig 5, depicting the nature of the slantwise and vertical circulations, is shown in Fig 7. The vertical arrows represent upright convection lifting air from close to the surface to 2.4 km just ahead of the SCF. The two bold inclined arrows represent the slantwise circulation, and the wavy line in between represents a shear zone. Fig 8 shows that this shear zone was associated with a coherent layer of low Richardson Number (Ri). Measured over 500 m (strictly 50 mb) layers, the minimum values of Ri were slightly less than 1. Coherent patterns were still achieved when Ri was evaluated over even shallower, 200 m layers (strictly 20 mb): within the dashed isopleths in Fig 8 the resulting Ri fell below the critical value of 0.25 for Kelvin-Helmholtz instability.

Clearly the convective cells were effective in mixing boundary layer air up to 2.4 km (and higher in parts of the front closer to the cyclone centre). What is not so clear is the role played by the shear layer in mixing boundary layer air into the free atmosphere. One's first impression is of the ascending branch of the slantwise circulation lofting boundary layer air into the free atmosphere. The fact that much of this flow (lightly stippled area in Fig 8), though close to saturation, was cloud-free suggests instead that the air within it originated from just above the boundary layer. Alternatively it might have consisted of some boundary layer air that was being diluted through mixing with dry air from the descending limb of the slantwise circulation. A close comparison of Fig 8 with Fig 5(c), however, shows that the layer with  $Ri < 0.25$ , though contiguous with, does not overlap with, the core of the rearward-directed flow, and so it appears unlikely that this mixing could account for the sub-saturation of the entire slantwise ascending flow.

We thus obtain a picture of a slantwise circulation in the form of a thinly laminated shear layer (vortex sheet) perturbing the top of the boundary layer. According to Browning et al (1994) the best defined of such vortex sheets correspond to the leading edges of fresh injections of dry intrusion air descending from upper levels, as seen in satellite water vapour imagery. The descending part of the slantwise circulation intrudes into the boundary layer and partially mixes dry air down to the surface just behind the SCF. The region of slantwise ascent lifts and pulls out a layer of air from the top of the boundary layer just ahead of the SCF. The region of slantwise ascent also starts to lift and pull out air from within the boundary layer but, at least in the present case, this realizes the potential instability and triggers shallow vertical convection. As a result, boundary layer air that otherwise would have ascended within the slantwise circulation or perhaps remained within the boundary layer, is vented vertically to a level where the flow is overtaking the front. At this level the cloudy air is detrained and may eventually create a new (higher) boundary layer top.

#### 4. Concluding remarks on some similarities in the structure of kata- and ana-cold fronts

In the introduction we described kata-cold fronts as being superficially different from ana-cold fronts. Certainly this author (Browning 1990) has represented them as two poles in a frontal classification scheme. This is still a valid perspective when viewing the fronts in terms of their broad-scale behaviour: thus the conceptual model of an ana-cold front in Fig 9 is clearly quite different from the model of a kata-cold front in Fig 1. However, we have shown in this paper that, when a kata-cold front is viewed on the mesoscale, it may be seen to have embedded within it the rudiments of a rearward-sloping circulation (Fig 7).

In an ana-cold front the boundary layer air is to a large extent peeled off into a strip of forced line convection before ascending slantwise to the rear. As a result of the wholesale peeling off of boundary layer air, there is an abrupt drop in surface temperature at such a front. In a kata-front the surface temperature drop tends to be smaller since only some of the boundary layer air is vented and only a fraction of this may undergo slantwise ascent. Yet the elements of an ana-cold frontal slantwise circulation may still be there. Evidently, therefore, it is not a discontinuous step for one kind of frontal circulation (kata) to evolve into another (ana): it is merely a matter of the slantwise circulation becoming quantitatively more intense and larger.

#### Acknowledgements

I am grateful to Clare Davitt for providing the dropsonde data and to the team led by Sid Clough who ran the FRONTS-92 experiment.

## References

- Browning, K.A. 1990: Organization of clouds and precipitation in extratropical cyclones. In 'Extratropical cyclones: the Erik Palmén Memorial Volume', C.W. Newton and E.O. Holopainen, Eds., American Meteorological Society, 129-153
- Browning, K.A., Clough, S.A., Davitt, C.S.A., Roberts, N.M. and Hewson, T.D. 1994: Observations of the mesoscale sub-structure in the cold air of a developing frontal cyclone. Submitted to Quart. J. Roy. Meteor. Soc.,
- Browning, K.A. and Monk G.A. 1982 A simple model for the synoptic analysis of cold fronts. Quart. J. Roy. Meteor. Soc., 108, 435-452
- Sansom, H.W. 1951 A study of cold fronts over the British Isles. Quart. J. Roy. Meteor. Soc., 77, 96-120

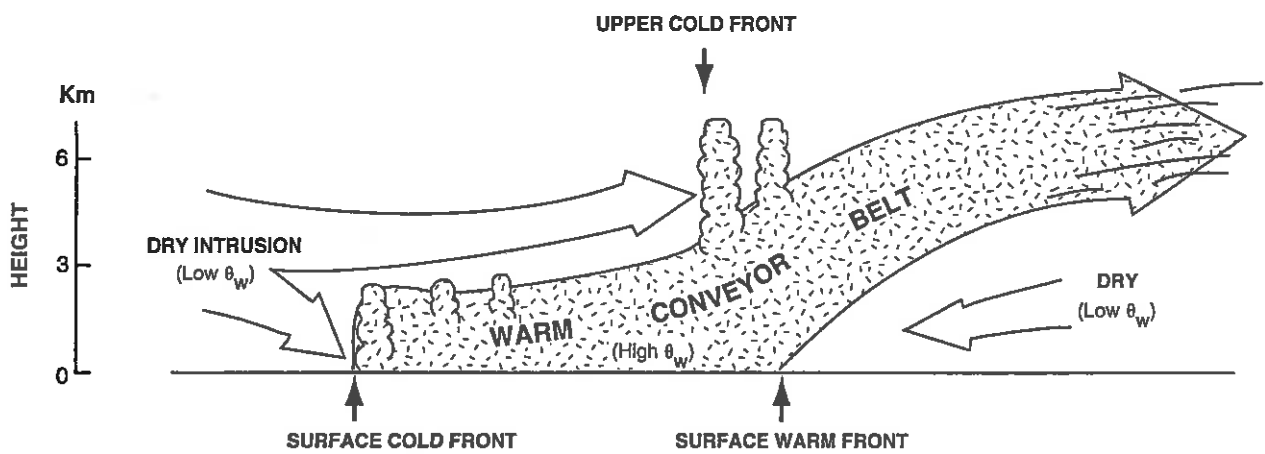


Fig. 1. Simple model of a kata-cold frontal situation in which dry air with low wet-bulb potential temperature ( $\theta_w$ ) overruns a shallow moist layer of high- $\theta_w$  air (Adapted from Browning 1990). The present paper is concerned with the mesoscale structure of the surface cold frontal region.

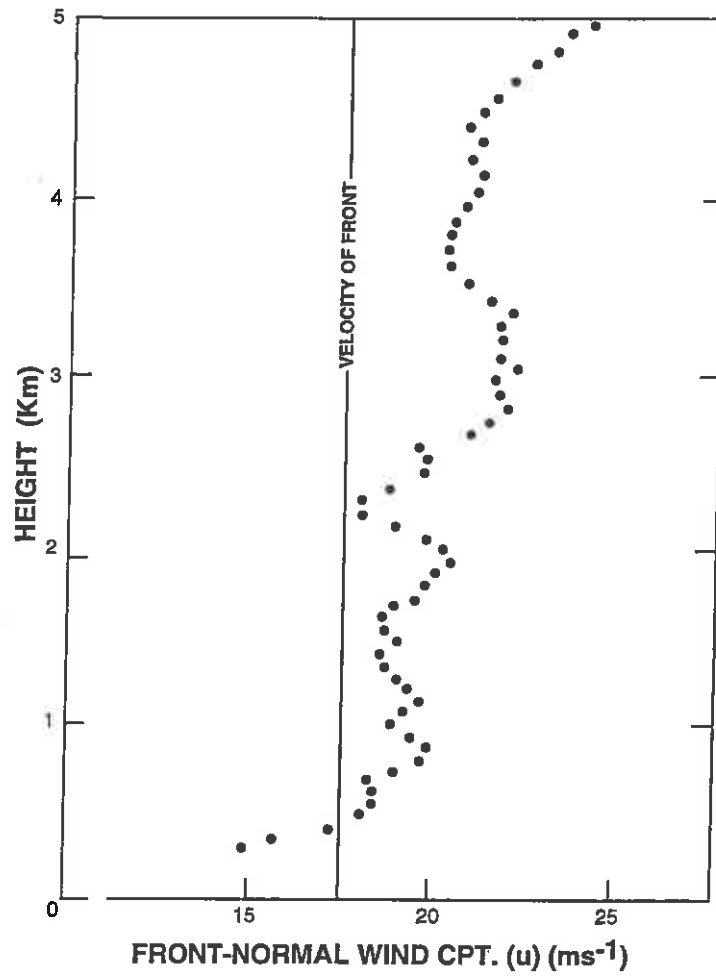


Fig. 2. Vertical profile of front-normal wind component (u) from Sounding Number 17 at location B in Fig 3.

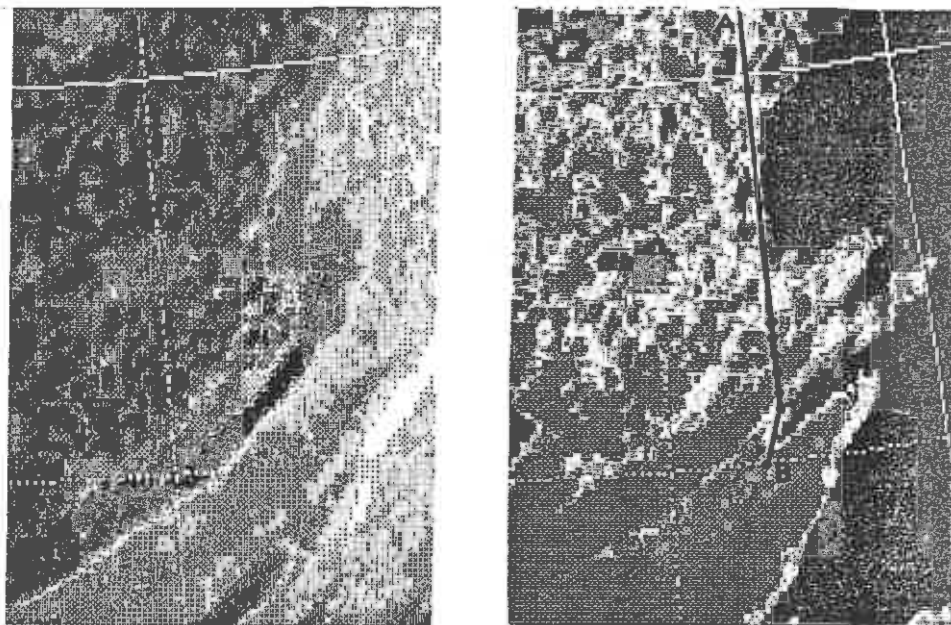


Fig. 3. Meteosat imagery showing cold frontal cloud bands at 1730 UTC, 27 April 1992: (a) visibility; (b) infra-red. Latitudes shown are  $45^{\circ}$  and  $50^{\circ}$ N; longitudes are  $10^{\circ}$  and  $15^{\circ}$ W. The grey scale in (b) is enhanced to reveal fine structure in the low cloud region (tops with temperatures between  $+5^{\circ}\text{C}$  and  $-3^{\circ}\text{C}$ ). AB is track of dropsonde aircraft; the nine dots at or near southern end of line are Sounding Numbers 11 to 19, as plotted in Figs 5 and 8.

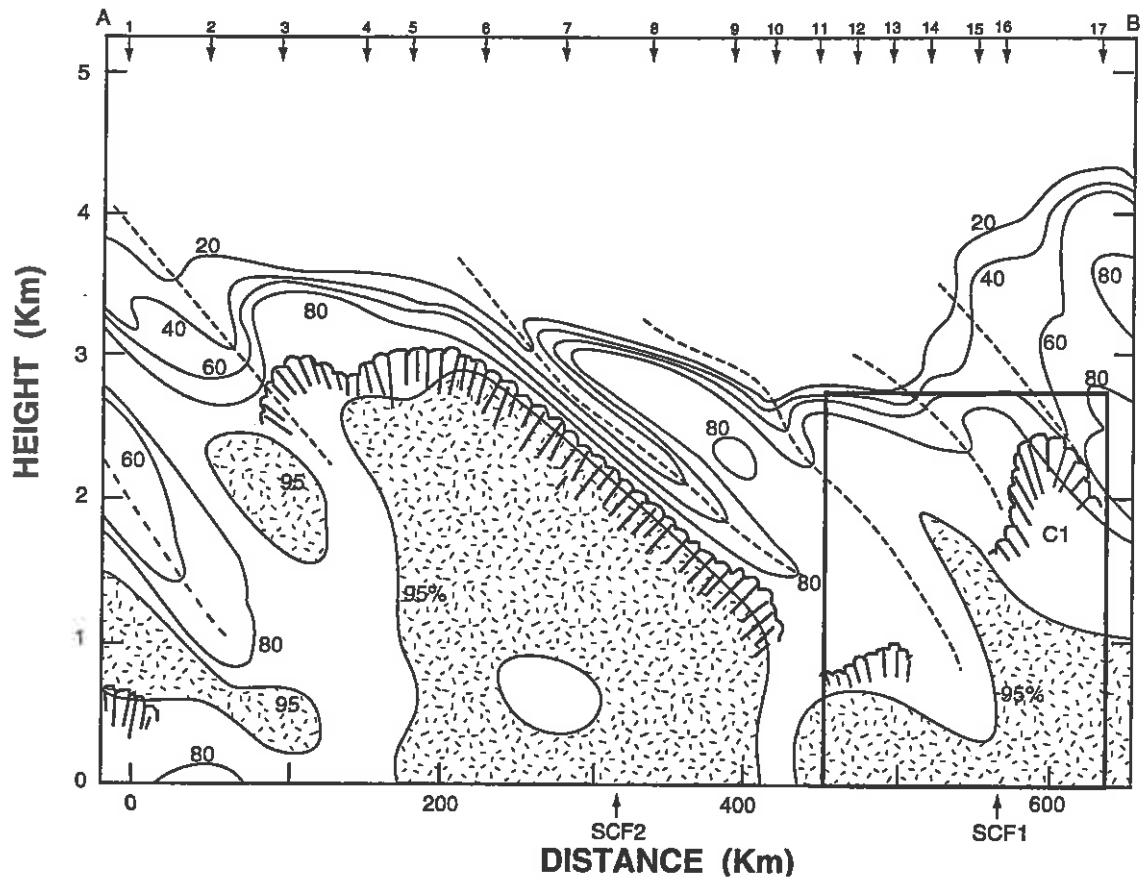


Fig. 4. Cross-section along AB (see Fig 3) showing isopleths of relative humidity superimposed upon outline of cloud tops derived from infra-red imagery. (After Browning et al 1994). Locations of Soundings 1-17 are identified at top of diagram. Most of this paper is concerned with the detailed analysis of SCF 1 within the framed (bottom right) part of the diagram.

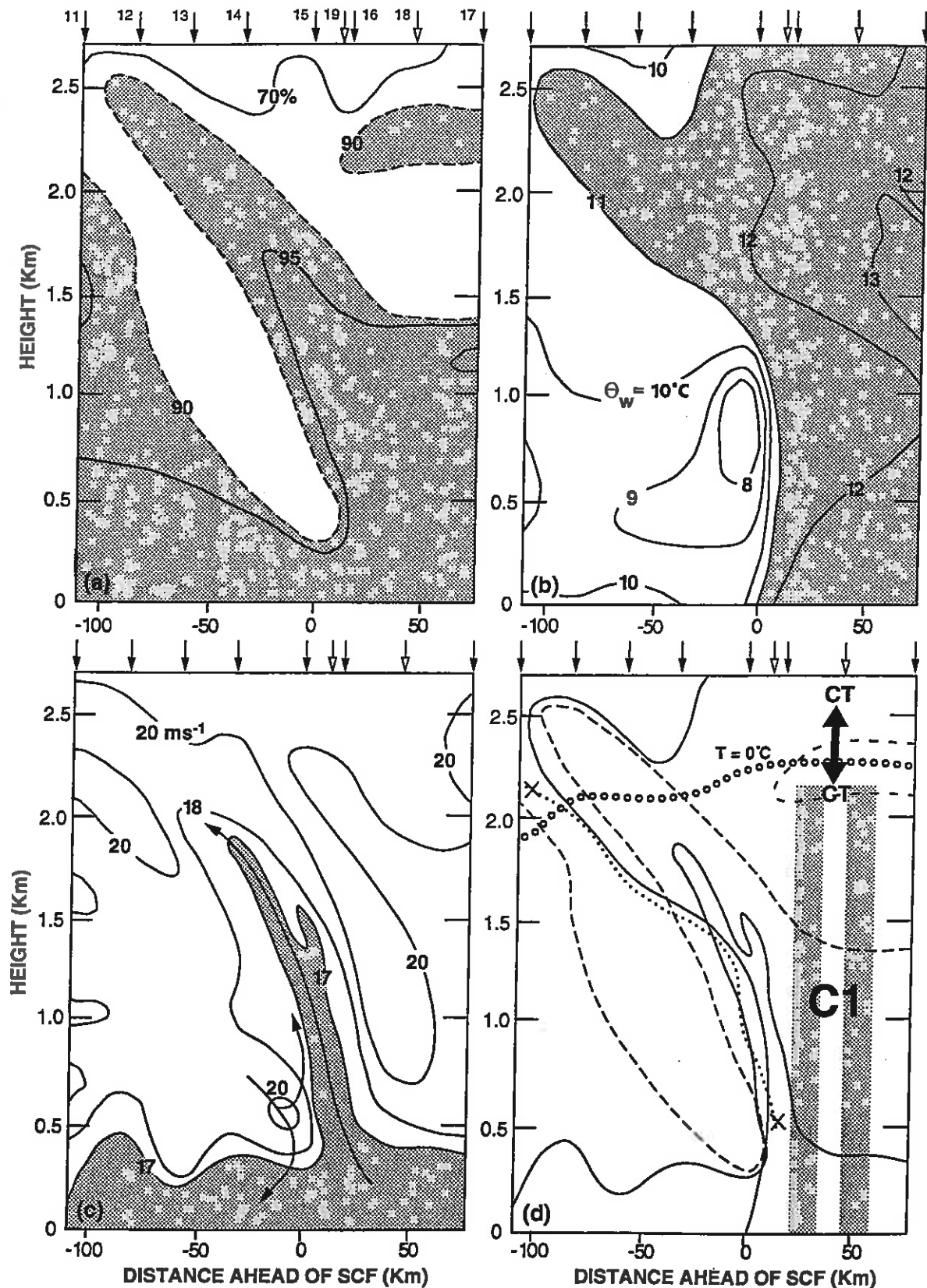


Fig. 5. Cross-section through SCF1 along southern part of AB (see Figs 3 and 4), based on Sounding Numbers 11 to 19 (see arrows at top of diagram). The 4 panels show: (a) relative humidity (isopleths at 70, 90 and 95%, shaded above 90%), (b) wet-bulb potential temperature,  $\theta_w$  (isopleths at 1°C intervals, shaded above 11°C), (c) front-normal wind component,  $u$ , (isopleths at 17, 18 and 20  $\text{m s}^{-1}$ , shaded below 17  $\text{m s}^{-1}$ ; velocity of front is between 17 and 18  $\text{m s}^{-1}$ ). (d) superposition of isopleths from (a), (b) and (c), the isopleths shown being those that bound the shaded regions in (a), (b) and (c). Also shown in (d) are the  $T=0^\circ\text{C}$  isotherm (line of circles), the axis of maximum vertical shear of the front-parallel wind component,  $dv/dz$  (dotted curve labelled XX), and the region of convective cloud C1 (shaded), the arrow labelled CT-CT giving an indication of uncertainty in the cloud-top height.

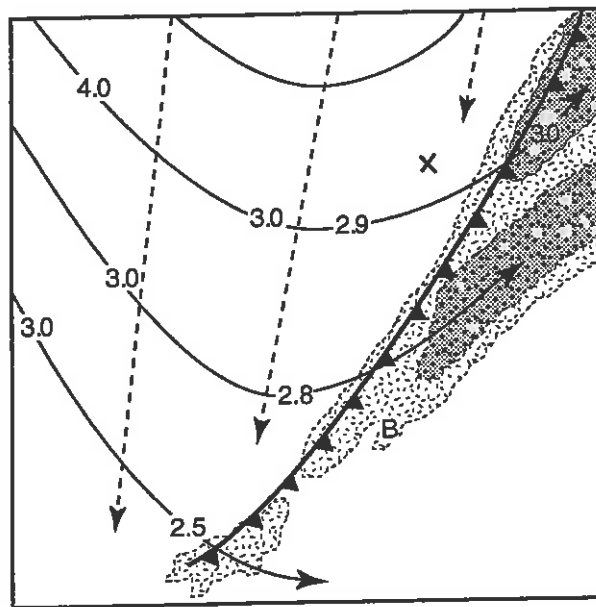


Fig. 6. Flow relative to SCF1 in the 10C and 25C isentropic surfaces (dashed and solid lines, respectively). The 10C flow descends from 1 km to the surface. Numbers along the 25C streamlines give heights in km. Cloud associated with SCF1 is also shown (low cloud is stippled; slightly higher cloud with tops to 2.4km is heavily stippled). XB marks the end points of the section in Fig 5.

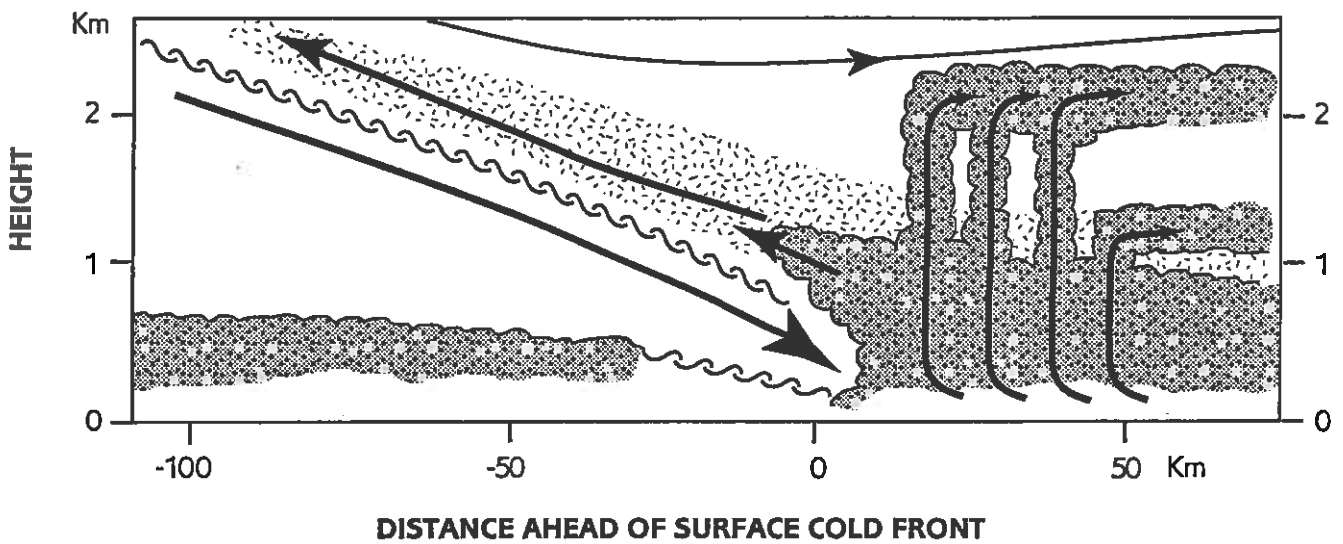


Fig. 7. Conceptual model of circulations at the surface cold front (SCF). Based on Figs 5 and 8 but stretched 4-fold to provide a more realistic aspect ratio. Cloudy boundary layer and ex-boundary layer air is stippled heavily. Vertical arrows ahead of the SCF represent convection. Inclined arrows behind the SCF represent slantwise ascent and descent on either side of a strongly sheared layer with low Richardson Number depicted by the wavy line. The lightly stippled layer above the wavy line represents a moist but unsaturated layer originating from just above the boundary layer.

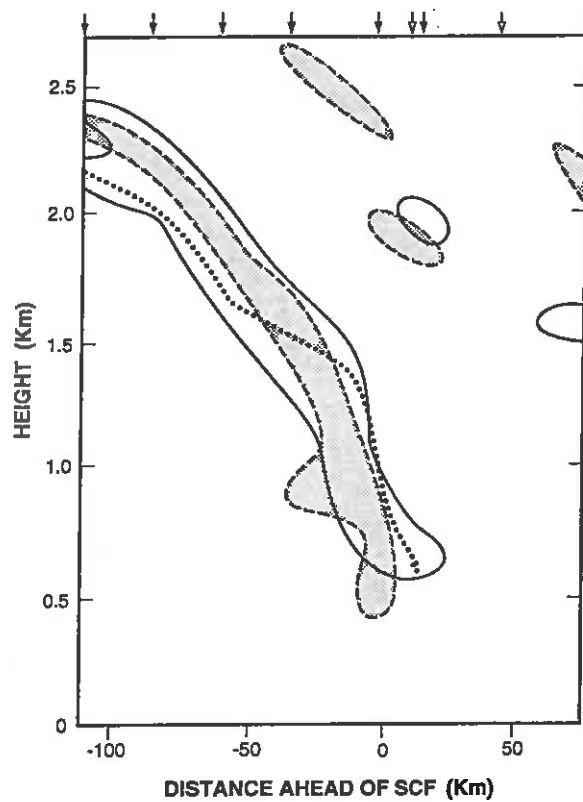


Fig. 8. Cross-section through SCF 1 as in Fig 5 but showing Richardson Number. The solid isopleth encloses regions where  $Ri < 1.0$  measured over 50 mb layers. The dashed isopleth encloses stippled regions where  $Ri < 0.25$  measured over 20 mb layers. The dotted line, taken from Fig 5(d), is the axis of maximum  $dv/dz$ .

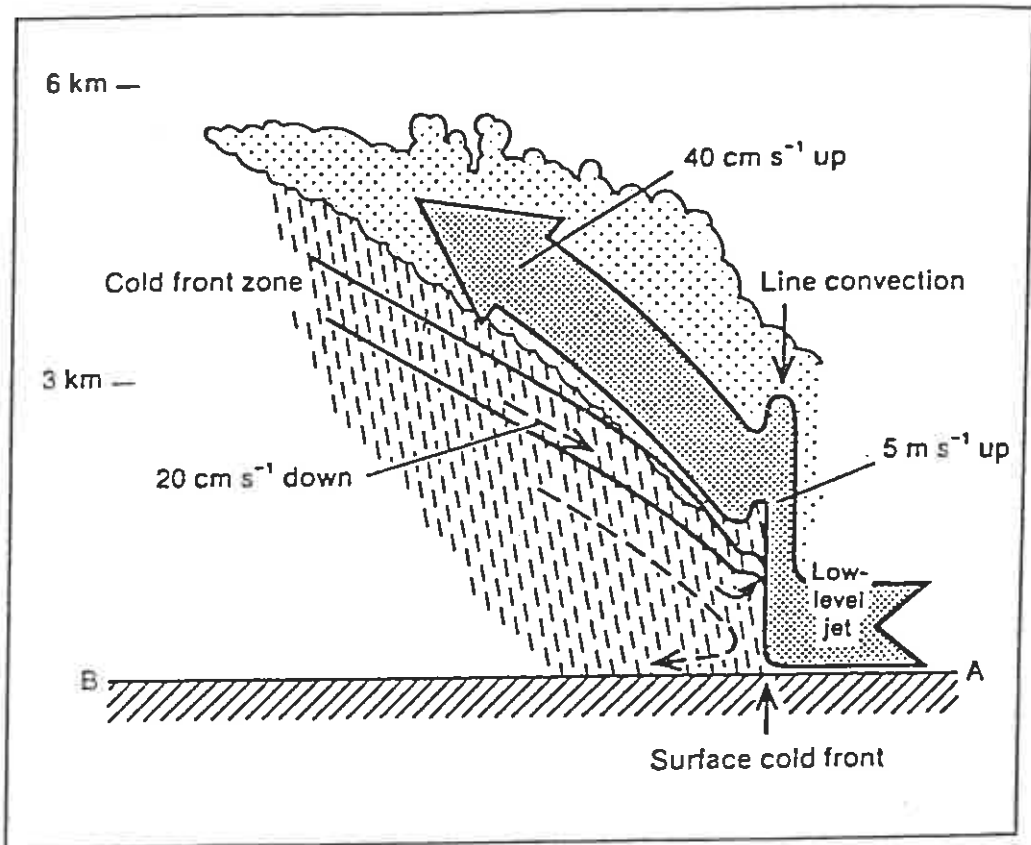


Fig. 9. Simple model of the airflow at an ana-cold front showing warm conveyor belt air with high  $\theta_w$  (bold arrow) originating at low levels ahead of the front and undergoing rearward-sloping ascent above descending air within the cold frontal zone. (From Browning 1990).

## CURRENT JCMM INTERNAL REPORTS

This series of JCMM Internal Reports, initiated in 1993, contains unpublished reports and also versions of articles submitted for publication. The complete set of Internal Reports is available from the National Meteorology Library on loan, if required.

1. **Research Strategy and Programme.**  
K A Browning et al  
January 1993
2. **The GEWEX Cloud System Study (GCSS).**  
GEWEX Cloud System Science Team  
January 1993
3. **Evolution of a mesoscale upper tropospheric vorticity maximum and comma cloud from a cloud-free two-dimensional potential vorticity anomaly.**  
K A Browning  
January 1993
4. **The Global Energy and Water Cycle**  
K A Browning  
July 1993
5. **Structure of a midlatitude cyclone before occlusion.**  
K A Browning and N Roberts  
July 1993
6. **Developments in Systems and Tools for Weather Forecasting.**  
K A Browning and G Szejwach  
July 1993
7. **Diagnostic study of a narrow cold frontal rainband and severe winds associated with a stratospheric intrusion.**  
K A Browning and R Reynolds  
August 1993
8. **Survey of perceived priority issues in the parametrizations of cloud-related processes in GCMs.**  
K A Browning  
September 1993
9. **The Effect of Rain on Longwave Radiation.**  
I Dharssi  
September 1993

10. **Cloud Microphysical Processes - A Description of the Parametrization used in the Large Eddy Model.**  
H Swann  
July 1994
11. **An Appreciation of the Meteorological Research of Ernst Kleinschmidt.**  
A J Thorpe  
May 1992
12. **Potential Vorticity of Flow Along the Alps.**  
A J Thorpe, H Volkert and Dietrich Heimann  
August 1992
13. **The Representation of Fronts.**  
A J Thorpe  
January 1993
14. **A Parametrization Scheme for Symmetric Instability: Tests for an Idealised Flow.**  
C S Chan and A J Thorpe  
February 1993
15. **The Fronts 92 Experiment: a Quicklook Atlas.**  
Edited by T D Hewson  
November 1993
16. **Frontal wave stability during moist deformation frontogenesis. Part 1. Linear wave dynamics**  
C H Bishop and A J Thorpe  
May 1993
17. **Frontal wave stability during moist deformation frontogenesis. Part 2. The suppression of non-linear wave development.**  
C H Bishop and A J Thorpe  
May 1993
18. **Gravity waves in sheared ducts.**  
S Monserrat and A J Thorpe  
October 1993
19. **Potential Vorticity and the Electrostatics Analogy: Quasi-Geostrophic Theory.**  
C Bishop and A J Thorpe  
November 1993
20. **Recent Advances in the Measurement of Precipitation by Radar.**  
A J Illingworth  
April 1993

21. **Micro-Physique et Givrage. Cloud Microphysics and Aircraft Icing.**  
A J Illingworth  
May 1993
22. **Differential Phase Measurements of Precipitation.**  
M Blackman and A J Illingworth  
May 1993
23. **Estimation of Effective Radius of Cloud Particles from the Radar Reflectivity.**  
N I Fox and A J Illingworth  
May 1993
24. **A Simple Method of Dopplerising a Pulsed Magnetron Radar.**  
L Hua, A J Illingworth and J Eastment  
November 1993
25. **Radiation and Polar Lows.**  
George C Craig  
February 1994
26. **Collected preprints submitted to International Symposium on the Life Cycles of Extratropical Cyclones; Bergen, Norway, 27 June - 1 July 1994**  
April 1994
27. **Convective Frontogenesis**  
Douglas J Parker and Alan J Thorpe  
April 1994
28. **Improved Measurement Of The Ice Water Content In Cirrus Using A Total Water Evaporator**  
Philip R A Brown and Peter N Francis  
April 1994
29. **Mesoscale Effects of a Dry Intrusion within a Vigorous Cyclone**  
K A Browning and B W Golding  
April 1994
30. **GEWEX Cloud System Study, Science Plan**  
May 1994
31. **Parametrization of Momentum Transport by Convectively Generated Gravity Waves**  
R Kershaw  
May 1994
32. **Mesoscale Modelling Newsletter, No. 5**  
May 1994

33. **Observations of the mesoscale sub-structure in the cold air of a developing frontal cyclone**  
K A Browning, S A Clough, C S A Davitt, N M Roberts and T D Hewson  
May 1994
34. **Longwave Radiative Forcing of a Simulated Tropical Squall Line**  
Imtiaz Dharssi  
July 1994

**Met Office** Joint Centre for Mesoscale Meteorology Department of Meteorology  
University of Reading PO Box 243 Reading RG6 6BB United Kingdom  
Tel: +44 (0)118 3778425 Fax: +44 (0)118 378 8791  
[www.metoffice.com](http://www.metoffice.com)

